Helium atom scattering from CO adsorbed at steps on Ni(001)

R. Berndt, B. J. Hinch, J. P. Toennies, and Ch. Wöll

Citation: The Journal of Chemical Physics **92**, 1435 (1990); doi: 10.1063/1.458102
View online: http://dx.doi.org/10.1063/1.458102
View Table of Contents: http://scitation.aip.org/content/aip/journal/jcp/92/2?ver=pdfcov
Published by the AIP Publishing

Helium atom scattering from CO adsorbed at steps on Ni(001)

R. Berndt,[a] B. J. Hinch, J. P. Toennies, and Ch. Wöll[b]
Max Planck Institut für Strömungsforschung, Bunsenstrasse 10, D 3400 Göttingen, Federal Republic of Germany

(Received 9 June 1989; accepted 8 September 1989)

Diffraction of helium atoms from randomly distributed step edges on the otherwise smooth (001) surface of Ni has been observed. Measurements for different azimuths near the ⟨100⟩ direction indicate that the step edges are lined up perpendicular to the ⟨100⟩ direction. The effect of CO adsorption on both the amplitude of the diffraction oscillations and also on specular scattering has been studied. The in-plane diffraction oscillations from the steps and the specular peak intensity show a similar attenuation with CO adsorption. This is interpreted in terms of a simple model for the effect of adsorption on the step diffraction oscillations. With increasing CO adsorption, the step edge diffraction patterns are also found to be slightly shifted suggesting a continuous change in step edge shape with adsorption.

1. INTRODUCTION

Helium atom scattering (HAS) has been demonstrated to be a versatile nondestructive, truly surface sensitive technique for the study of the structure and dynamics of clean and adsorbate covered surfaces.[1] Because the atomically smooth surfaces of low-indexed metal single crystals reflect almost totally in the specular direction any type of defect can be easily observed in the scattering. Just as in the interaction of He atoms with free molecules, the potential describing this interaction is governed by a long-range attractive and a short-range repulsive potential.[2] Thus the specular intensity and the scattering at small angles, with respect to the specular peak, is dominated by the long-range attractive potential, whereas the scattering at larger angles is determined by the repulsive potential of short range. Both measurements of the specular intensity[3] and large angle scattering[4,5] have been successfully used to study defects such as adatoms and steps on surfaces.

The attenuation of the specular intensity by a single adatom or admolecule is characterized by a total cross section of the order of several tens to hundreds of Å^2.[6,7] All deflections contribute, even those due to small momentum transfers produced by a long-range attractive potential. Thus, coverages of only 10^{-4} monolayer can lead to a 1% attenuation of the specular beam and can be detected. A similar sensitivity to steps has also been reported.[8] When measured as a function of incident angle and/or energy the specular intensity shows regular undulations.[9] These are attributed to interference between neighboring terraces separated by steps. Thus, the amplitudes of oscillations can be used to determine average step heights and densities. Moreover, information on adsorbate diffusion to step sites has been derived from the exposure time evolution of the specular intensity.[10] Details on the actual "shape" of the defects themselves, however, cannot be extracted from this data since the decrease in the specular intensity cannot distinguish between the different final deflections of the scattered He atoms.

With the increased dynamic range of experimental apparatuses, it has become possible to measure the large angle diffuse elastic scattering from single defects on otherwise smooth metal single-crystal surfaces.[4,5] Such experiments are more difficult because of the much lower intensities amounting typically to less than about 10^{-4} of the specular intensity. The weak features can only be observed on the otherwise smooth metal surfaces [e.g., (111) and (001) faces of fcc crystals] since the diffraction intensities on these surfaces are very small so that they do not mask the weak structures. Widely spaced interference oscillations have been observed in the scattering from single, randomly distributed steps on Pt(111),[5] Al(111),[11] Cu(111),[12] and Fe(110).[13] It has been shown that these interference oscillations can provide detailed information of the helium atom-surface potential in the vicinity of the step edge.[14] Interference oscillations have also been observed in the scattering from single chemisorbed CO molecules[4] on Pt(111). The energy width of these diffusely scattered elastic intensities are found to be the same as that of the incident beam. However, on a Pb(110) surface close to the melting point, where these weak diffuse intensities are also seen, the peaks have been found to be broadened in energy. This broadening or quasielastic scattering has also recently been shown to provide direct information on the diffusion coefficient and the atomic mechanism of defect diffusion.[15]

In the present investigation, we have studied both small (near specular) and large angle He atom scattering from a CO-covered randomly stepped Ni(001) surface, as a function of CO exposure. The CO/Ni(001) system has been extensively investigated in connection with the nickel catalyzed methanation reaction ($3H_2 + CO \rightarrow CH_4 + H_2O$).[16] Although the structure and phase diagrams have been extensively studied[17] there is only indirect evidence from experiments with the synthesis of $Ni(CO)_4$ on single crystal faces for the importance of step sites.[18,19]

The experimental specular intensity shows the expected

[a] Present address: IBM Forschungslabor, Säumerstrasse 4, CH 8803 Rüschlikon, Switzerland.
[b] Present address: Institut für Angewandte Physikalische Chemie, Universität Heidelberg, Im Neuenheimer Feld 253, 6900 Heidelberg, Federal Republic of Germany.

 0021-9606/90/021435-07$03.00

exponential attenuation upon CO adsorption and serves as a monitor of the adsorbate density on terraces. The shape, positions, and intensities of the large angle diffraction oscillations determine the effects of CO on the step sites. The observations are analyzed with a theoretical diffraction model based on a hard wall scattering potential. The theoretical analysis suggests that preferential CO adsorption at step edges may not be as strong as suggested by a more simple analysis.

II. EXPERIMENTAL

The apparatus is essentially similar to one described in detail in Ref. 20 and modified for studies of metal surfaces as described in Ref. 21. A high pressure ($\approx$100 atm) nozzle (10 μm diameter) is used to generate an intense and monochromatic beam of helium atoms. The energy of the beam can be varied from about 8 meV ($k_i = 4$ Å^{-1}) to 65 meV ($k_i = 11$ Å^{-1}) by changing the source temperature from 40 to 300 K, respectively, and has a relative energy spread [full width at half-maximum (FWHM)] of about 2% over this range. The crystal is mounted on a high resolution homemade triple axis manipulator. The electron bombardment, magnetic mass spectrometer detector is located at the end of a 1.2 m flight tube which, for the purposes of this experiment, was fixed at an angle $\theta_{SD} = 90°$ with respect to the incident beam. In this arrangement, only helium atoms scattered with incident and final angles $\theta_i + \theta_f = \theta_{SD}$ are detected. Angular intensity distributions are measured simply by the rotation of the crystal about an axis perpendicular to the scattering plane. The change in parallel wave vector is zero for specular, elastic scattering ($\theta_i = \theta_f = 45°$) and, for other in-plane conditions, is given by

$$\Delta K = k_f \sin\theta_f - k_i \sin\theta_i, \tag{1}$$

where k_i and k_f are the magnitudes of the incident and final wave vectors.

The measurement of the weak intensities at large ΔK, described in the present paper, requires a dynamic range in sensitivity of at least five orders of magnitude. This is achieved as described in Ref. 20 by using a large diffusion pump (12 000 l/s) at the source and extensive differential pumping between source, target, and the mass spectrometer detector. The large source pump enables the generation of very intense beams and the differential pumping ensures that the helium partial pressure in the detector chamber can be kept below 10^{-15} Torr, resulting in a background of less than 10 counts/s.

The nickel crystal was cut to within 0.25° of the (001) face and, after initial mechanical polishing, was cleaned in vacuum by cycles of annealing at 1200 K and neon ion bombardment. Traces of remaining carbon were removed by heating the crystal in oxygen followed by further cycles of bombardment and annealing. After this additional procedure, the cylindrical mirror Auger-analyzer (PHI Model 10-155) trace showed no observable impurities. More quantitatively, all impurity Auger features (e.g., oxygen, carbon, or sulphur) were each less than 1% of a monolayer. The clean surface showed very weak He diffraction peaks amounting to 2×10^{-4} of the specular beam intensity at $k_i = 11.2$ Å^{-1}.

The stepped surface is prepared by ion bombardment and subsequent partial annealing following the same procedure as described in Ref. 22. Using this procedure, monatomic steps are found oriented along the ⟨100⟩ directions and with randomly distributed terrace sizes. Step edges were also found along ⟨110⟩ directions, but were not the subject of study here.

The carbon monoxide was adsorbed by exposing the crystal to an ambient CO pressure in the 10^{-9} Torr range at a temperature of 300 K for a defined length of time. CO is known to be molecularly adsorbed on nickel below 350 K.[23] Absolute coverages were estimated by using the appearance of additional helium diffraction peaks at $\Delta K = 1.78$ Å^{-1} along the ⟨100⟩ azimuth to indicate an ordered $c(2\times2)$ phase at half a monolayer as a reference point. The $c(2\times2)$ overlayer was found to be well formed after an exposure of 3.5 L. Higher exposures resulted in the formation of a compressed structure, as observed previously.[24] Time-of-flight spectra reveal in addition to the surface phonon peaks, new inelastic peaks with $\Delta E = \pm 3.5$ meV, which are attributed to the excitation of the low energy, hindered translational mode of the adsorbed molecule.[25] In these measurements the total specular intensity, denoted by I_0 throughout, was typically $\sim 8\times10^6$ counts per second. The signal was quite stable over long periods except for an initial small decrease of the order 5% over the measurement time for an entire angular distribution (typically 18 min) due to a slow, but gradual contamination of the surface.

III. RESULTS

A. Scattering data for the clean, randomly stepped surface

Figure 1 shows two angular distributions of helium elastically scattered from the clean nickel surface. The angular dependence has been converted to a momentum transfer dependence by the use of Eq. (1) for ΔK with $k_f = k_i$. Note that the relative intensity scale is logarithmic. The lower trace shows the distribution obtained at $\phi = 0°$ along the ⟨100⟩ azimuth at a surface temperature of 300 K and $k_i = 11.2$ Å^{-1}, corresponding to a beam energy of 65.8 meV. At parallel momentum transfers greater than $\Delta K \sim 2.0$ Å^{-1}, there are three broad maxima at about 1.5 Å^{-1} intervals. In principle these features might be due to either incoherent elastic scattering from defects, or inelastic scattering from phonons. The latter possibility has been investigated by examining the time-of-flight spectra at small angles as shown in the inset of Fig. 1. The falloff of the inelastic contribution with increasing parallel momentum transfer is very sharp, as is to be expected.[2] The first order diffraction peaks are 2×10^{-4} smaller than the specular peak. Since inelastic intensities, which are dominated by single phonon events, are proportional to the diffraction intensities the inelastic contributions can be safely neglected at ΔK greater than the Brillouin zone boundary at 1.78 Å^{-1}. Thus the oscillations in intensity at larger parallel momentum transfers can be attributed to incoherent elastic scattering from defects.

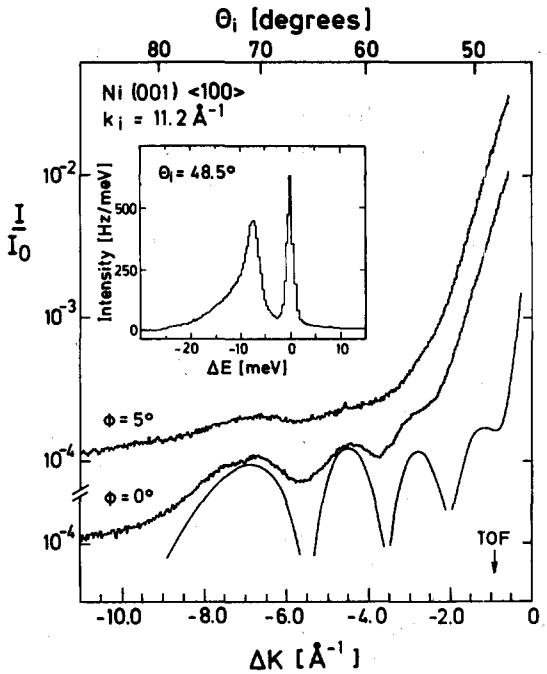

FIG. 1. The total scattered intensity, from a room temperature Ni(001) crystal, as a function of parallel momentum transfer, for two different azimuths. All data is for $k_i = 11.2$ Å^{-1}. The uppermost curve is taken for an azimuth 5° removed from the ⟨100⟩ azimuth. The central curve displays the results of an angular scan exactly at the ⟨100⟩ azimuth. The lowest curve is the result of calculations along the ⟨100⟩ azimuth from a model hard wall potential representing infinitely extended step edge defects. The parameters for this model are as follows: steepest angle of descent = 34°; step width $W = 5.7$ Å; and step density $\rho = 1/250$ Å^{-1}. The result of a time-of-flight energy analysis is shown in the inset. This example was taken at $\theta_i = 48.5°$ and is indicated on the parallel momentum axis. The top scale shows the conversion of the incident angles to parallel momentum transfers.

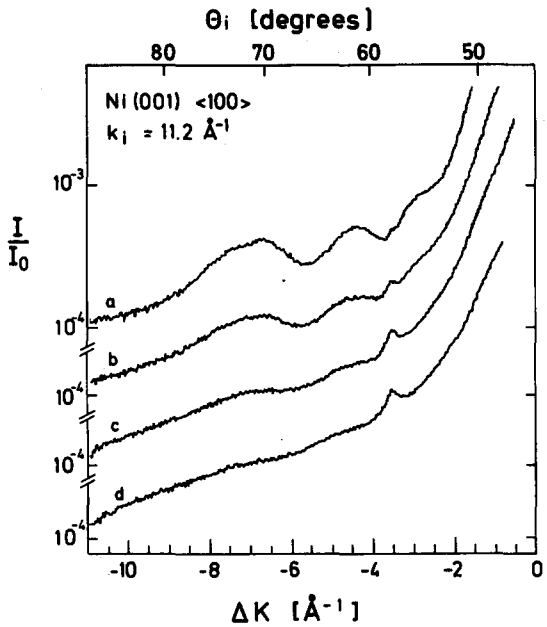

FIG. 3. Diffusely scattered intensity along the ⟨100⟩ azimuth of the Ni(001) crystal. $k_i = 11.2$ Å^{-1}. The scans are taken at varying CO exposures: (a) 0.0 L; (b) 0.5 L; (c) 1.5 L; and (d) 2.5 L. All intensities are relative to the specular intensity at zero exposure.

These defects could be either point defects, which include single adatoms, vacancies, or adsorbed molecules, or line defects such as step edges. In the former case, the scattered intensity should be largely independent of the azimuthal angle.[4] The upper trace in Fig. 1 demonstrates that rotating the ⟨100⟩ azimuth by 5° out of the scattering plane reduces the oscillation amplitude to a fraction of its maximum value. This demonstrates that these observed oscillations are due to extended linear defects produced by step edges oriented normal to the ⟨100⟩ azimuth.[26] The finite azimuthal width of about 5° (FWHM) of the oscillations is caused by the limited distances between kinks or other defects in the step edges which limit the average coherence length in the azimuthal direction. We can estimate the coherence length and the width in parallel momentum space along the ⟨100⟩ direction to be about 10 and 0.6 Å^{-1}, respectively. For the later discussion of the apparent scattering cross sections of CO molecules, it is important to note that these features are very much broader in ΔK space than the specular or diffraction peaks. This is shown in Fig. 2, which is a schematic diagram constructed from the available data.

B. Scattering data for the CO covered randomly stepped surface

Subsequent to the characterization of the clean surface the same crystal was exposed to varying amounts of CO. Figure 3 shows the angular distributions measured for successively increased CO exposures of 0.5, 1.5, and 2.5 L at a crystal temperature of 300 K. From the calibration of the sticking coefficient, based on the appeareance of the $c(2\times2)$

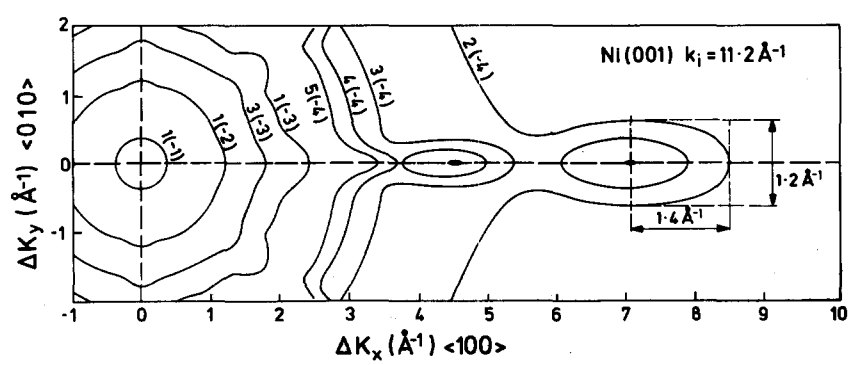

FIG. 2. A schematic contour plot of intensities observable from the Ni(001) surface, demonstrating diffuse scattering from step edges along ⟨100⟩ and ⟨010⟩ azimuths. All numbers are with respect to specular (maximum) intensity. ($-n$) denotes $\times 10^{-n}$.

diffraction peaks (see Sec. II), the corresponding coverages are estimated to be $\theta = 0.07$, 0.2, and 0.3 monolayers, respectively. Careful examination of Fig. 3 reveals a number of interesting observations. First, we note that the magnitude of the interference oscillations decreases with increasing exposure. This contrasts with the appearance of a new somewhat sharper peak, with increasing exposure, at $\Delta K = -3.56$ Å^{-1}. The location of this peak coincides with that of the first-order diffraction peak, which is only barely visible for the clean surface. Next we note that the background signal has also increased significantly. This can be most clearly seen by comparing the signals at $\Delta K = -10$ Å^{-1} which increases proportionally with exposure.

A more qualitative analysis of the data is possible by subtracting the unstructured background from the angular distributions. The smooth background I_{bg} arises predominant from phonon and multiphonon excitation processes and was assumed to have locally a parabolic distribution. Figure 4 shows the remaining angular distribution after subtracting off the background. Note that the intensity scales have been multiplied by the indicated factors to facilitate comparison of the structures. Moreover, we have not included the first oscillation at about $\Delta K \cong -3$ Å^{-1} since it appears to be noticeably perturbed by the first-order peak at -3.6 Å^{-1}. To reduce the noise, while sacrificing some of the angular resolution, the distributions (c) and (d) have been smoothed by taking a sliding average over three and five channels, respectively. Only the average value at the central channel is plotted.

This presentation of the data reveals new features not so readily apparent in Fig. 3. It is now seen that both peaks are shifted to somewhat larger momentum transfers with increasing CO adsorption. The shift is best seen for the peak at about $\Delta K \cong -7$ Å^{-1}. The shifts are plotted separately in Fig. 5. There is also some evidence for partially unresolved structure at the maximum of the $\Delta K = -7$ Å^{-1} peak, which is especially apparent in (a) and (d). Unfortunately, because of the poor statistics in (d), the structures observed there cannot be regarded as significant, whereas the structure in the peak of curve (a) probably is. It should be noted, however, in passing that the structures coincide roughly with the expected location of the second-order diffraction peak at $\Delta K = -7.12$ Å^{-1}. In an analogous experiment on the clean Pt(111) surfaces,[5] similar splitting of the maxima was also seen in diffraction oscillations coinciding with a diffraction peak for the smooth surface. This splitting has been explained by an enhanced atomic corrugation in the vicinity of the step edge.[14] (See note added in proof.)

The shifts in the peak locations plotted in Fig. 5 are of the order of 0.4 Å^{-1} and are well within the resolution of our apparatus which is about $\pm 0.1°$, corresponding to an uncertainty in ΔK of about 0.03 Å^{-1} at this incident energy. The shift cannot be attributed to changes in the beam energy since the weak diffraction peak at $\theta_i = 58.1°$ remains at the same angular position to within much less than 0.2°. The largest conceivable changes in k_i can therefore not be greater than ~ 0.1 Å^{-1} and consequently cannot be responsible for the magnitude of the observed shifts.

Finally in Fig.6, we compare the decrease in the intensities of the diffusely diffracted peaks with that of the specular

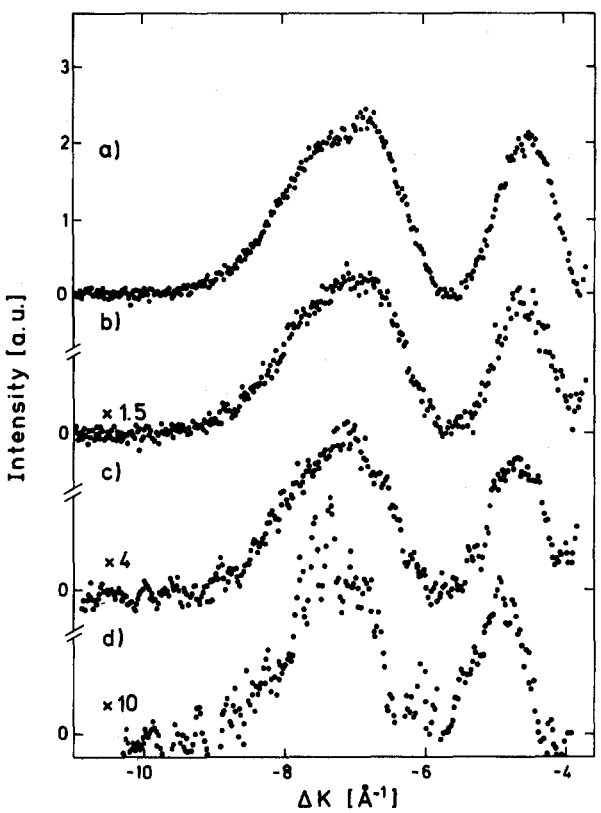

FIG. 4. The data of Fig. 3 on a linear intensity scale and after the subtraction of the background contribution. CO exposures are as follows: (a) 0.0 L; (b) 0.5 L; (c) 1.5 L; and (d) 2.5 L. Only the two peaks at largest parallel momentum transfer are shown. The peak positions move to larger $|\Delta K|$ with increasing CO coverage.

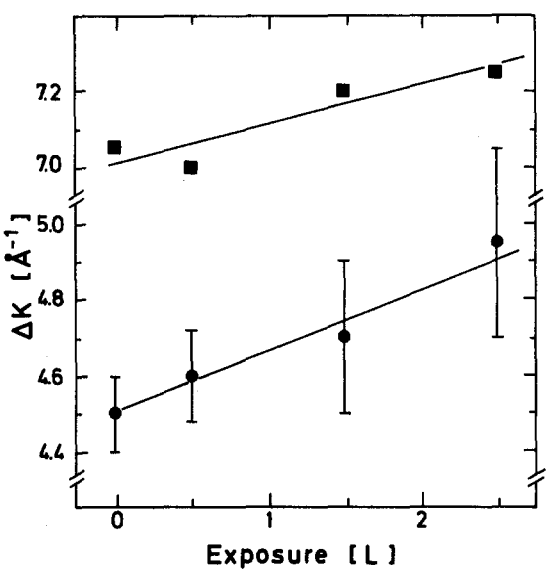

FIG. 5. Positions of peaks from the scans of diffusely scattered intensity from step edges. The CO exposure is expressed in Langmuirs. $k_i = 11.2$ Å^{-1} scattering along the ⟨100⟩ azimuth.

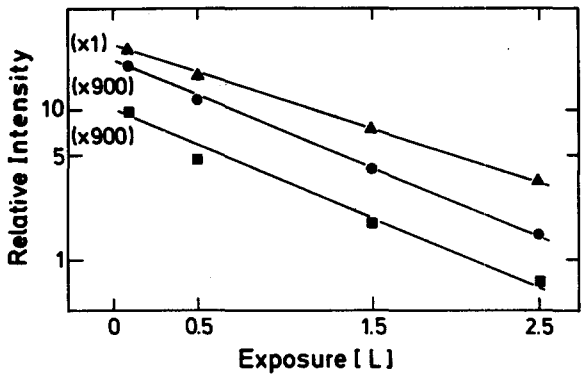

FIG. 6. The relative integral intensities of peaks in the angular scans as a function of CO exposure, after background subtraction. The three observed peaks are specular (triangles) that centered at $\Delta K \simeq 4.7$ Å^{-1} (squares) and that centered at $\Delta K \simeq 7.1$ Å^{-1} (dots).

peak intensity, as a function of CO exposure. Surprisingly, the intensities of both experiments have about the same relative exponential decrease. From the initial decrease of the specular peak and the coverage calibration, the integral cross section for scattering from randomly distributed CO on Ni(001) is determined to be about 170 Å^2. This value is about a factor of 2.5 larger than the value of Ibanez, Garcia, and Rojo who obtained 65 Å^2.[7] The difference can be explained by the fact that these authors assumed a sticking coefficient of one, whereas from our calibration it appears that the sticking coefficient is closer to about 0.3.

IV. DISCUSSION

The oscillations observed in the angular distributions of He scattering from the clean surface along the ⟨100⟩ symmetry direction shown in Fig. 1 have been fitted to a potential profile for a single step in the hard wall Eikonal approximation. The calculational procedure is the same as that described in Ref. 14. The best fit angular distribution, shown in Fig. 1, is calculated for a step width of $W = 5.7$ Å and a steepest angle of the potential of $\epsilon_{max} = 34°$ with respect to the surface plane. From the amplitude of the oscillations relative to the specular peak, the average step density is determined to be about 0.004 Å^{-1}. The step edge parameters can be compared with previous determinations of step profiles using the same procedure for other surfaces. Along the ⟨112⟩ azimuth of Pt(111), values of $W = 6.6$ Å and $\epsilon_{max} = 38°$ were found for $k_i = 9.7$ Å^{-1} which are very similar to the values found for Al(111) step edges, at $k_i = 9.6$ Å^{-1}; $W = 6.4$ Å and $\epsilon_{max} = 37°$. The step edge parameters are only weakly dependent on the incident energy. It is interesting to note that the smaller width observed for Ni(001) is consistent with the smaller step heights of $h = 1.76$ Å for Ni(001) compared to $h = 2.27$ Å for Pt(111) and to $h = 2.34$ Å for Al(111).

On CO adsorption at 300 K, the distributions, at large angles, reveal the following three separate phenomena: (i) the appearance of a Bragg peak with intensity increasing with gas exposure; (ii) an outward shift in the location of the oscillations proportional to the CO exposure which is accompanied by (iii) a decrease in the absolute intensity of diffusely scattered oscillations similar to the decrease in the specular peak.

The observation of the first-order Bragg peaks at $\Delta K = 3.56$ Å^{-1} indicates that the adsorbate molecules are adsorbed at equivalent sites on the surface and thereby form a lattice gas. This has also been observed in low-energy electron diffraction (LEED) measurements.[17] At these exposures of CO on Ni(001), we do not expect completion of the known $C(2\times2)$ phase which corresponds to a coverage of half a monolayer ($\theta = \frac{1}{2}$). If the CO were to form islands of $c(2\times2)$, we would expect intensities of the half-order peaks which are comparable to the magnitudes of the first-order diffraction peaks. For the 0.5, 1.5, and 2.5 L exposures, the half-order peaks are not observed. This suggests that there is no island formation and certainly no long range $c(2\times2)$ type order of the CO molecules at these coverages.

The observations (ii) and (iii) above are more difficult to explain. For simplicity we will treat the two effects separately, thus discussing first the shift in terms of a step profile which is uniform along the ⟨010⟩ direction of the step. Using the same hard wall eikonal approximation as for the clean surface, we find that the outward shift of the oscillations by about 0.4 Å^{-1} corresponds to a decrease in the step width by about 0.3 Å or 5% in the overall width. Thus the observations indicate that the step edge becomes more abrupt with CO exposure.

If we assume that the CO molecules at the step edge sites lead predominantly to a scattering of the He atoms out of the sagittal plane, then the change in step profile must be attributed to the step edge regions between the CO molecules. We also note that CO on Ni(001) leads to a substantial increase in the work function amounting to 0.31 eV for 1 L.[23] Such an increase in the work function at the step edges would tend to decrease the range of the electron spillout, into the vacuum, shifting the repulsive part of the potential closer in towards the surface planes. This in turn would imply that the equipotentials follow more closely the step edges. The effective hard wall position would follow a sharper or steeper line and the effective width of the single step edges would be reduced. In this model the increase in work function could be due to CO molecules at the step edges and/or widely separated on the terraces.

The change in oscillation amplitude with exposure, in relation to the change in specular intensity, provides valuable information on the relative occupancy of step sites vs terrace sites. Previously we found only a small attenuation of the large angle oscillations on Al(111) relative to specular intensities with O_2 adsorption.[11] The relative attenuation was comparable with that observed here with CO adsorption on the Ni(001) surface. The observations are, however, contrary to the large attenuation with CO adsorption on Pt(111).[3] Attenuation of the specular beam due to random adsorption of atoms or molecules can be treated in a straightforward manner by the application of Beer's law, which states that at low coverages the attenuation depends exponentially on the large integral cross section of the defect. The large cross sections result from small momentum transfers imparted by the long-range attractive potential of the adsorbed molecule. A similar law should describe the attenu-

ation of the step-related diffuse peaks.

As opposed to the interpretation of the attenuation of the specular peak, there are a number of problems which make the interpretation less straightforward:

(i) The most important is that the step diffraction peaks are broad. This broadening leads to a considerable correction of the cross sections for reasons that will be discussed later.

(ii) The scattering cross section for atoms in the vicinity of steps will be different from those residing on terraces. For one they will be partly shielded by the steps and/or kinks. Moreover, it is possible that they will be slightly distorted because of the stronger interactions at the step or kink sites.

(iii) Finally, any theory will have to take into account the possibility that the positions of the adsorbed molecules are correlated with step edges. The assumption of a random distribution made in approximate theories of scattering from molecules on terraces is less likely to be valid. Because of the reduced dimensionality of step edges, any correlation would be more significant.

If we neglect effects (ii) and (iii), we can at first expect the integral cross sections to be considerably smaller than for the specular scattering from terraces. A much larger angular deflection is required to scatter out of the broad diffuse peak. A very rough estimate would be to assume a kinetic gas cross section (e.g., $\sigma \approx \pi R_0^2$), where R_0 is the hard sphere radius for the scattering at steps. Such cross sections are typically of the order of 30–40 Å^2 compared to the much larger total integral cross sections discussed above. Thus the cross sections for the step related diffuse peaks could be about an order of magnitude smaller. If this is the case, then the similar attenuation observed for the specular and diffraction peaks would suggest that there is an order of magnitude preference for step sites.

If we look more deeply into effect (i) above, then this simple model can be looked upon as giving only an order of magnitude estimate of the effective cross section. In lieu of an exact theory which would go far beyond the scope of this paper, Appendix A sketches out a rough argument in support of this.

An accurate analysis, which would take account of the arrangement of the adsorbed molecules relative to the step edges, is needed in order to make a reliable estimate of the probabilities of step vs terrace adsorption. At present, we realize that corrections to the simple classical estimates of the cross sections for attenuation of the step-related diffraction maxima relative to the attenuation of the specular peak are required. Thus the apparent experimental evidence for a strong preference of adsorbates for step sites must be regarded with caution.

V. SUMMARY

The present experiments on the effect of chemisorbed molecules on diffuse scattering from steps open up new possibilities for the direct study of adsorption. The experiments have demonstrated for the first time that CO molecules adsorbed on the Ni(001) surface have a large effect on the observed attenuation of the diffuse intensities. Moreover, we have observed a shift in diffraction intensity oscillations. Since the diffuse scattering is sensitive to the repulsive potential energy profile of the step, a change in this profile in regions not occupied by CO molecules is indicated. When a full analysis is available, the techniques demonstrated here will provide detailed information on the site specificity of the adsorption process in relation to step edges and on the effect of adsorption on the structure of steps.

Note added in proof: More recent work indicates that the splitting seen on clean Pt(111) is more likely due to coherent diffraction arising because of lattice gas correlations of the step sites (J. Hinch and J. P. Toennies, Submitted to Phys. Rev. B; C. W. Skorupka and J. R. Manson, submitted to Phys. Rev. B).

ACKNOWLEDGMENTS

The authors would like to thank J. R. Manson, V. Celli, and J. Frenken for many fruitful discussions. One of us (B. J. H.) thanks the Alexander von Humboldt foundation for a stipendium.

APPENDIX A: A DISCUSSION OF THE EFFECTIVE CROSS SECTIONS FOR DIFFUSE PEAKS

In general, the intensity $I(\mathbf{K})$, as a function of the parallel momentum exchange vector $\mathbf{K}$, is given by

$$I(\mathbf{K}) \propto |A(\mathbf{K})|^2, \tag{A1}$$

where $A(\mathbf{K})$ is the scattering amplitude. In the simplest Eikonal approximation,[27] A can be expressed in terms of a corrugation function $\zeta(\mathbf{R})$ and the perpendicular component of the incident wave vector k_i^z:

$$A(\mathbf{K}) \propto \int \exp(-i\mathbf{K}\cdot\mathbf{R})\exp[-i2k_i^z\zeta(\mathbf{R})]\,d\mathbf{R}. \tag{A2}$$

Now consider the effect of the adsorption on ζ. Let $\zeta^0(\mathbf{R})$ be the corrugation of the surface including step defects, but without adsorbates. Ignoring effect (ii) of Sec. IV, then the corrugation with adsorbates will be

$$\zeta(\mathbf{R}) = \zeta^0(\mathbf{R}) + \sum_{j=1}^{n} h(\mathbf{R}-\mathbf{R}_j), \tag{A3}$$

where $\mathbf{R}_j$ denotes the set of n adsorption sites. The height function $h(\mathbf{R})$ is centered on each adsorbate and in principle may extend over a length scale of order of 20 Å or more. Hardwall correction functions over such a length scale are required to imitate the effect of the long-range attractive contributions to the interaction potential. The height functions have also been assumed to be purely additive. Substituting Eq. (A3) into Eq. (A2), we get the scattering amplitude as a convolution of two isolated functions

$$A(\mathbf{K}) = A^0(\mathbf{K}) * A_a(\mathbf{K}), \tag{A4}$$

where A^0 represents the scattered amplitude from the adsorbate free surface

$$A^0(\mathbf{K}) \propto \int \exp(-i\mathbf{K}\cdot\mathbf{R})\exp[-i2k_i^z\zeta^0(\mathbf{R})]\,d\mathbf{R} \tag{A5}$$

and

$$A_a(\mathbf{K}) \propto \int \exp(-i\mathbf{K}\cdot\mathbf{R}) \prod_j \exp[-i2k_i^z h(\mathbf{R}-\mathbf{R}_j)]\,dR. \tag{A6}$$

$A_a(\mathbf{K})$ thus contains all the information on the adsorbate cross sections and their positions on the substrate and with respect to each other. Equation (A4) above is applicable to all intensity peaks in K space, be they diffuse intensity oscillations, or specular from the surface.

Normally, a cross section for an adsorbate refers to the attenuation of specular scattering from a surface. This is exactly analogous to cross sections in the gas phase. In contrast to the attenuation of a specular peak, the diffuse peaks have their centers at $K = K_d$, where $K_d \neq 0$ and are relatively broad in K space. The first of these two basic differences is relatively unimportant. However, the attenuation of the peak maximum is affected by the fact that the width of the diffuse peaks may now be larger than that of the adsorbate related function A_a. The attenuation is dependent on the phase characteristics of $A_a(\mathbf{K},\theta)$. In the attenuation of specular scattering, the variation of phase in A_a is unimportant since the peak is necessarily very sharp (or delta function-like).

In the past it has been assumed that the intensities follow a convolution, i.e.,

$$I(\mathbf{K}) = I^0(\mathbf{K}) * I_a(\mathbf{K}) \tag{A7}$$

in analogy to Eq. (A4). The intensity functions I, I^0, and I_a are all real functions of $\mathbf{K}$:

$$I^0(\mathbf{K}) = |A^0(\mathbf{K})|^2 \tag{A8}$$

and

$$I_a(\mathbf{K}) = |A_a(\mathbf{K})|^2. \tag{A9}$$

$I_a(\mathbf{K})$ describes classically the set of possible deflections on an otherwise well-defined atom trajectory due to scattering from randomly distributed adsorbates. Equation (A7) is thus a classical description of the decrease in height and broadening of diffraction peaks with low concentrations of adsorbates. Quantum effects are accounted for within the Eikonal approximation and lead to Eq. (A4). Generally Eqs. (A4) and (A7) are not equivalent,

$$|A^0(\mathbf{K})|^2 * |A_a(\mathbf{K})|^2 \neq |A^0(\mathbf{K}) * A_a(\mathbf{K})|^2. \tag{A10}$$

Equation (A7) is true for specular, or any $I^0(\mathbf{K})$ function that consists only of sharp diffraction peaks.

Thus, we have shown that arguments involving only the classical idea of scattering and deflection using Eq. (A7) do not necessarily provide an accurate estimate of the effective cross sections of adsorbates on diffuse intensity peaks.

[1] J. P. Toennies, J. Vac. Sci. Technol. A **5**, 440 (1987).
[2] D. Eichenauer, U. Harten, J. P. Toennies, and V. Celli, J. Chem. Phys. **86**, 3693 (1987).
[3] G. Comsa and B. Poelsema, Appl. Phys. A **38**, 153 (1985).
[4] A. M. Lahee, J. R. Manson, J. P. Toennies, and Ch. Wöll, J. Chem. Phys. **86**, 7194 (1987).
[5] A. M. Lahee, J. R. Manson, J. P. Toennies, and Ch. Wöll, Phys. Rev. Lett. **57**, 471 (1986); **57**, 2331 (1986).
[6] See, e.g., B. Poelsema, S. T. de Zwart, and G. Comsa, Phys. Rev. Lett. **49**, 578 (1982).
[7] J. Ibañez, N. Garcia, and J. M. Rojo, Phys. Rev. B **28**, 3164 (1983).
[8] L. K. Verheij, B. Poelsema, and G. Comsa, Surf. Sci. **162**, 858 (1985).
[9] J. Lapujoulade, Surf. Sci. **108**, 526 (1981).
[10] B. Poelsema, L. K. Verheij, and G. Comsa, Phys. Rev. Lett. **49**, 1731 (1982).
[11] A. Lock, Diplomarbeit, Göttingen, Federal Republic of Germany (1986).
[12] B. J. Hinch, A. Lock, J. P. Toennies, and G. Zhang J. Vac. Sci. Technol. (in press).
[13] J. P. Toennies, Ch. Wöll, and G. Zhang (in preparation).
[14] B. J. Hinch, Phys. Rev. B **38**, 5260 (1988).
[15] J. W. M. Frenken, J. P. Toennies, and Ch. Wöll, Phys. Rev. Lett. **60**, 1727 (1988).
[16] D. W. Goodman, R. D. Kelley, T. E. Madey, and J. T. Yates, Jr., J. Catal. **63**, 226 (1980).
[17] G. Andersson and J. B. Pendry, J. Phys. C **13**, 3547 (1980).
[18] P. de Groot, M. Coulon, and K. Dransfeld, Surf. Sci. **94**, 204 (1980).
[19] D. B. Liang, G. Abend, J. H. Block, and N. Kruse, Surf. Sci. **126**, 392 (1983).
[20] G. Lilienkamp and J. P. Toennies, J. Chem. Phys. **78**, 5210 (1983).
[21] J. P. Toennies, J. Vac. Sci. Technol. A **2**, 1055 (1984).
[22] B. Poelsma, L. K. Verheij, and G. Comsa, Phys. Rev. Lett. **53**, 2500 (1984).
[23] D. E. Eastman and J. Cashion, Phys. Rev. Lett. **27**, 1520 (1971).
[24] J. C. Tracy, J. Chem. Phys. **56**, 2736 (1972).
[25] R. Berndt, J. P. Toennies, and Ch. Wöll, J. Electron. Spectrosc. **44**, 183 (1987).
[26] Close packed step edges normal to the ⟨110⟩ directions should be the more stable of the two orientations. However, we have not observed the scattering normal to the ⟨110⟩ directions in conjunction with CO adsorption.
[27] U. Garibaldi, A. C. Levi, R. Spadacini, and G. E. Tommei, Surf. Sci. **48**, 649 (1975).